1996

# Modeling magnetostrictive microstructure under loading : and, Simulation of magnetoelastic systems

Richard James
*Carnegie Mellon University*

David Kinderlehrer

Ling Ma

NAMT
96-004

# Modeling Magnetostrictive Microstructure Under Loading

Richard James
University of Minnesota

David Kinderlehrer and Ling Ma
Carnegie Mellon University

# Simulation of Magnetoelastic Systems

David Kinderlehrer and Ling Ma
Carnegie Mellon University

**Research Report No. 96-NA-004**

**March 1996**

**Sponsors**

**U.S. Army Research Office
Research Triangle Park
NC 27709**

**National Science Foundation
1800 G Street, N.W.
Washington, DC 20550**

# Modeling Magnetostrictive Microstructure Under Loading

Richard James

Department of Aerospace Engineering and Mechanics
University of Minnesota
Minneapolis, MN 55455

David Kinderlehrer and Ling Ma

Center for Nonlinear Analysis
Carnegie Mellon University
Pittsburgh, PA 15213-3890

and

# Simulation of Magnetoelastic Systems

David Kinderlehrer and Ling Ma

Center for Nonlinear Analysis and Department of Mathematics
Carnegie Mellon University
Pittsburgh, PA 15213-3890

$$W(RFH, mR^T, x) = W(F, m, x) \quad \text{for } R \in SO(3) \text{ and } H \in \mathbb{H}_x,$$

where $\mathbb{H}_x$ is the symmetry group of the material at $x \in \Omega$. In our case, $\mathbb{H}_x$ will be the proper cubic group $\mathbb{H}$ of order 24 or one of its conjugacy classes.

In Terfenol-D, onset of ferromagnetism is associated with a stretch of the high temperature cubic unit cell along a main diagonal, inducing a magnetization parallel to that diagonal. Thus the energy density $W$ for a single crystal achieves its minimum on the eight pairs of transformation strains $(U_i, \pm m_i)$ given by

$$U_i = \eta_1 1 + (\eta_2 - \eta_1)\, m_i \otimes m_i, \quad 0 < \eta_1 < \eta_2, \quad i = 1,2,3,4, \tag{1.3}$$

$$m_1 = \frac{1}{\sqrt{3}}(1,1,1), \quad m_2 = \frac{1}{\sqrt{3}}(-1,1,1), \quad m_3 = \frac{1}{\sqrt{3}}(1,-1,1), \quad m_4 = \frac{1}{\sqrt{3}}(1,1,-1).$$

This leads to

$$W(RU_j, m_j R^T) = W(RU_1 H, m_1 R^T) = \min W, \quad R \in SO(3), \ H \in \mathbb{H}, \ j = 1,2,3,4.$$

As suggested in Figure 1, the typical configuration of $TbDyFe_2$ rods is a twinned dendritic structure consisting of lamellar domains separated by grain boundaries or growth twin interfaces. The entire rod is viewed as a composite, that we take here to be one domain $\Omega^+ = \{ x \cdot m_1 > 0 \} \cap \Omega$ and a second one $\Omega^- = \{ x \cdot m_1 < 0 \} \cap \Omega$. The lower lamellar structure arises as a rotation of $180^\circ$ about the $m_1$ axis of the original upper lattice. Denoting by $R_o$ this rotation, we arrive at an energy density of the composite given by

$$W(F, m, x) = \begin{cases} W(F, m) & x \in \Omega^+ \\ W(FR_o, m) & x \in \Omega^- \end{cases} \tag{1.4}$$

Note that $R_o$ is not a symmetry element of the original energy and, although holding invariant the wells of $(U_1, \pm m_1)$, gives a different set of transformation strains and magnetizations $(U'_i, \pm m'_i) = (R_o U'_i R_o, \pm m_i R_o)$.

We may now investigate the collection of twinned dendritic equilibrium structures corresponding to $H = 0$. From theory ([23,24]), we know that a minimizing sequence $(y^k, m^k)$ giving rise to such a configuration must satisfy

$$\int_\Omega W(\nabla y^k, m^k, x)\, dx + \frac{1}{2} \int_{R^3} |\nabla_y u^k|^2\, dy \to \min W\, |\Omega|$$

For the Young measure $\nu = (\nu_x)_{x \in \Omega}$ generated by $(\nabla y^k, m^k)$, we then have that

$$\int_\Omega \int_{M \times S^2} W(A, \mu, x)\, d\nu_x(A, \mu) dx = \min W\, |\Omega|, \text{ and} \tag{1.5}$$

$$\operatorname{div}_y \bar{m} = 0 \quad \text{where} \quad \bar{m} = \int_{M \times S^2} \mu\, d\nu_x(A, \mu)$$

and $M$ denotes the set of $3 \times 3$ matrices. This determines the variational condition for the support of the measure $\nu$, namely

$$\operatorname{supp} \nu_x \subset \Sigma^+ = \{(RU_i, \pm m_i R^T): R \in SO(3), i = 1,2,3,4\} \text{ for } x \in \Omega^+ \text{ and}$$



$$\operatorname{supp} \nu_x \subset \Sigma^- = \{(RU'_i, \pm m'_i R^T): R \in SO(3), i = 1,2,3,4\} \text{ for } x \in \Omega^- \tag{1.6}$$

The twinned dendritic laminates are the Young Measures with the simple form

$$\nu_x = \begin{cases} \frac{1}{2}(1-\lambda)(\delta_{(M,m)} + \delta_{(M,-m)}) + \frac{1}{2}\lambda(\delta_{(N,q)} + \delta_{(N,-q)}) & x \in \Omega^+ \\ \frac{1}{2}(1-\lambda')(\delta_{(M',m')} + \delta_{(M',-m')}) + \frac{1}{2}\lambda'(\delta_{(N',q')} + \delta_{(N',-q')}) & x \in \Omega^- \end{cases} \tag{1.7}$$

where $(M,m), (N,q) \in \Sigma^+$ and $(M',m'), (N',q') \in \Sigma^-$.

We confine our attention to the deformation gradients alone. It then follows from the minors relations that we are reduced to solving an algebra problem for macroscopic deformation gradients $F$ composed of matrices $M$ and $N$ and $F'$ composed of matrices $M'$ and $N'$ which satisfy

$$\begin{aligned} &F = (1-\lambda)M + \lambda N \text{ and } F' = (1-\lambda')M' + \lambda' N', \quad 0 \le \lambda, \lambda' \le 1, \\ &M - N = \alpha \otimes n, \quad M' - N' = \alpha' \otimes n', \quad \text{and} \\ &F' - F = b \otimes m_1 \end{aligned} \tag{1.8}$$

where $(M,m), (N,q) \in \Sigma^+, (M',m'), (N',q') \in \Sigma^-$

| *variants* | *twin planes* | *intersection of twin plane with (0–11)* |
|---|---|---|
| 1 2 | (100) twin | ⟨011⟩ |
| | (011) reciprocal | ⟨100⟩ |
| 1 3 | (010) twin | ⟨100⟩ |
| | (101) reciprocal | ⟨–111⟩ |
| 14 | (001) twin | ⟨100⟩ |
| | (110) reciprocal | ⟨–111⟩ |
| 23 | (001) twin | ⟨100⟩ |
| | (110) reciprocal | ⟨111⟩ |
| 34 | (–100) twin | ⟨011⟩ |
| | (01–1) reciprocal | parallel to ⟨01–1⟩ |
| 24 | (0–10) twin | ⟨100⟩ |
| | (10–1) reciprocal | ⟨111⟩ |

Table 1. Twinning data for the compatible variants. The third column gives the intersection of the twin plane with the (0–11) plane of observation

The middle line above is the twinning equation for the individual laminates subject to the constraint that (1.5) holds. The transformation strains (1.3) determine a coherent well structure: any pair of wells admits two lamellar configurations, and hence 12 in all for each of $\Omega^+$ and $\Omega^-$. Combining these, there are 144 possible combinations satisfying the middle line of (1.8), but imposing the condition of coherence across the growth twin boundary, which is the last line of (1.8), reduces these to twelve. They must have $i = k$, $j$

and in this case, $q$ is a normal direction for the interface between the two systems, either coarse or fine phase in our Young Measure sense.

The choice $q = (0,1,0)$ has the property

$$Qm_1 = -m_3 \text{ and } Qm_2 = m_4.$$

Note incidentally that since $n \cdot q = 0$, $Qn = -n$ and the normal direction is preserved. Now

$$QU_1Q = U_3 \text{ and } QU_2Q = U_4,$$

so by choosing $R^\dagger$ appropriately, we may solve (3.3). Thus a transformation path may be
found and moreover, the interface normal is $(0,1,0)$, independent of the volume fraction $\lambda$. For further discussion of the compatibility between different systems of variants and connections with experiment, see Tickle [36].

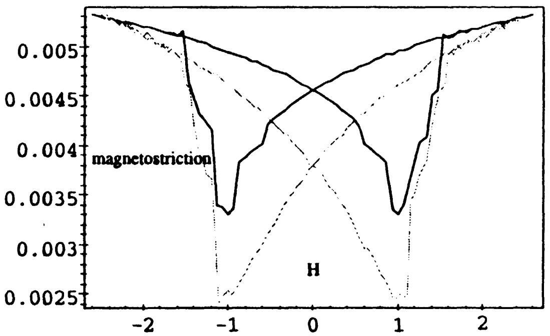


Figure 2. Computed hysteresis curves for a laminate (gray lower curve) and for a laminate with constrained growth twin interface and under compression (black upper curve).

Actual device performance under magnetic loading shows hysteretic behavior. Simulations have been employed to capture this phenomena, [27,28,29], and open the issue of the nature of metastable magnetic configurations. For a description of the experimental magnetostrictive curve we refer to Clark [14] and the references there. Metastability from the experimental, computational, and analytical points of view is an active topic of research we we do not have space to review here. We wish to remark only that the ability to produce a reliable and robust hysteresis curve by applying a general numerical method, like the conjugate gradient method, to a nonconvex functional was unanticipated and has led to some new ideas for analyzing such curves.

The simulation which gives rise to Figure 2 is based on linear theory in two dimensions but includes the magnetostatic energy term. The curve corresponding to the constrained growth twin interface more closely resembles the experimental picture, suggesting a role for the growth twin in the magnetostrictive process which to date is not clearly understood.

On the other hand, the width of the hysteresis loop seems to be relatively insensitive to loading or constraints. Indeed, additional simulations under a wide variety of conditions, for example, without magnetic field energy or elasticity or single crystals with magnetic field energy, suggest that the width of the curve is extremely robust. The simulation which



gives Figure 2 is the first, to our knowledge, where competition between magnetic and elastic effects is prominent.

## References


[1] Al-Jiboory, M., and Lord, D.G., 1990, Study of the magnetostrictive distortion in single crystal terfenol-D by x-ray diffraction, IEEE Trans Mag 26, 2583-2585.

[2] Al-Jiboory, M., and Lord, D.G., Bi, Y.J., Abell, J. S., Hwang, A.M.H., and Teter, J.P., Magnetic domains and microstructural defects in Terfenol-D, J. Appl. Phys. (to appear).

[3] Ball, J.M. and James, R.D. 1987 Fine phase mixtures as minimizers of energy, Arch. Rat. Mech. Anal. 100, 13-52.

[4] Ball, J.M. and James, R.D. 1991 Proposed experimental tests of a theory of fine microstructure and the two well problem, Phil. Trans. Roy. Soc. Lond. A338, 389-450

[5] Ball, J.M., Chu, C., James, R.D. 1994 Metastability of Martensite, preprint.

[6] Bhattacharya, K. 1991 Wedge-like microstructure in martensite, Acta Metall Mater 39, 2431-2444.

[7] Bhattacharya, K. 1992 Self accomodation in martensite, Arch. Rat. Mech. Anal. 120, 201-244.

[8] Bhattacharya, K., Firoozye, N., James, R., and Kohn, R. 1994 Restrictions on microstructure, Proc. R. Acad. Edin., 124A, 843-878

[9] Brown, W.F. 1963 Micromagnetics, John Wiley and Sons.

[10] Brown, W.F. 1966 Magnetoelastic Interactions, Vol. 9 of Springer Tracts in Natural Philosophy (C. Truesdell, ed.), Springer-Verlag.

[11] Chipot, M., and Kinderlehrer, D. 1988 Equilibrium configurations of crystals, Arch. Rat. Mech. Anal. 103, 237-277.

[12] Chu, C., James, R.D., and Kinderlehrer, D., (to appear).

[13] Clark, A. E. 1980 Magnetostrictive rare earth - Fe2 Coumpounds, Ferromagnetic Materials, Vol 1 (Wohlfarth, E.P., ed) North Holland, 532-589.

[14] Clark, A. E. 1995 High power magnetistrictivematerials from cryogenic temperatures to 250 C, Materials for Smart Systems, (George, E. P., Takahashi, S., Trolier-McKinstry, S., Uchino, K., and Wun-Fogle, M., eds.) Mat. Res. Soc. Vol. 360,171-182

[15] Clark, A. E., Verhoven, J.D., McMasters, O.D., and Gibson, E.D. 1986 Magnetostriction of twinned [112] crystals of Tb.27Dy.73Fe2, IEEE Trans Mag. 22, 973-975.

[16] DeSimone, A. 1993 Energy minimizers for large ferromagnetic bodies, Arch. Rat. Mech. Anal. 125, 99-143.

[17] DeSimone, A.. Magnetoelastic solids: macroscopic response and microstructure evolution under applied magnetic fields and loads, J. Intel. Mat. Sys. Structures (to appear).

[18] Dooley, J. and DeGraef, M. 1995 TEM study of twinning and magnetic domains in Terfenol-D,Materials for Smart Systems, (George, E. P., Takahashi, S., Trolier-McKinstry, S., Uchino, K., and Wun-Fogle, M., eds.) Mat. Res. Soc. Vol. 360, 189-194

[19] Ericksen, J.L. 1987 Twinning of crystals I, Metastability and Incompletely Posed Problems, (S. Antman, J.L. Ericksen, D. Kinderlehrer, I. Müller,eds) IMA Vol. Math. Appl. 3, Springer, 77-96.

[20] Ericksen, J.L. 1991 On kinematic conditions of compatibility, J. Elas. 26, 65-74.

[21] James, R. and Kinderlehrer, D. 1989 Theory of diffusionless phase transitions, PDE's and continuum models of phase transitions, (Rascle, M., Serre, D., and Slemrod, M., eds.) Lecture Notes in Physics 344, Springer, 51-84.

[22] James, R. and Kinderlehrer, D. 1990 Frustration in ferromagnetic materials, Continuum Mech. and Thermodynamics 2, 215-239.

[23] James, R. and Kinderlehrer, D. 1992 Frustration and Microstructure: an example in magnetostriction, Progress in PDE, calculus of variations, applications (Bandle, et al., eds) Pitman Res. Notes Math 267, 59-81.

[24] James, R. and Kinderlehrer, D. 1993 Theory of magnetostriction with application to TbxDy1−xFe2, Phil. Mag. B, 68, 237-274

[25] James, R. and Kinderlehrer, D. 1994 Theory of Magnetostriction with application to Terfenol-D, J. Appl. Phys., 76, 7012-7014

[26] James, R.D., and Müller, S. 1994 Internal variables and fine scale oscillations in micromagnetics, Continuum Mech. Thermodyn. 6.

[27] Kinderlehrer, D. and Ma, L. 1994 Computational hysteresis in modeling magnetic systems, IEEE Trans Mag.,30.6, 4380-4382

[28] Kinderlehrer, D. and Ma., L. The hysteretic event in magnetic systems, Nonlinear analysis(to appear).

Proc. SPIE Mathematics and Control in Smart Structures 1996
vol. 2715 (V. Varadan, ed.)

# Simulation of Magnetoelastic Systems

David Kinderlehrer and Ling Ma

Center for Nonlinear Analysis and Department of Mathematics
Carnegie Mellon University
Pittsburgh, PA 15213-3890

**Abstract** The simulation of a magnetoelastic system subjected to magnetic field loading gives rise to hysteresis. Examples related to Terfenol-D are presented and some methods of analysis discussed.

KEYWORDS magnetoelastic system, Terfenol-D, simulation, magnetostriction, metastability, micromagnetic theory

## 1. Introduction

We discuss the simulation of the behavior of a magnetoelastic system under magnetic field loading. Our principle objective is to understand the magnetostrictive curve of Terfenol-D, $Tb_xDy_{1-x}Fe_2$, $x \approx 0.3$, from the viewpoint of micromagnetic theory, [3,4,9,14,15-19]. Simulations of magnetic, magnetostrictive, and pseudoelastic behavior exhibit hysteresis, [20-23]. These systems have a highly nonlinear character involving both short range anisotropy and elastic fields and dispersive demagnetization fields. The hysteretic character of a simple system that moves quasistatically is robust. The energy profile in terms of applied magnetic field, and in particular, the width of the hysteresis loop, is invariant under mesh refinement. This is true even in the absence of an imposed dynamical mechanism, like the Landau-Lifschitz-Gilbert equation. This permits us, for example, to extract useful information by computing on fairly coarse grids. It is also very efficient, running at an excess of 200 MFLOPS on the Pittsburgh Supercomputing Center Cray C90. A typical simulation involves 600 to 800 field steps, each one of which represents a complete conjugate gradient iteration procedure. For experimental observations and theory we refer to [1,2,5-7,13]. Instabilities in Terfenol films are studied in Wuttig et al. [27].



An important feature of this type of simulation is that computed states are only metastable. Indeed, since the energy of configurations on loading and unloading are different for the same value of the imposed magnetic field, not both and usually neither can be minima. Little is known to guide us about metastability in this context. In addition, Terfenol displays a complicated lamellar microstructure whose role in the magnetostrictive process remains under investigation, [26]. Although confirming our ability to determine general features of the magnetization and magnetostriction, our results do not accurately describe the microstructure. So there is much room for improvement. However, we would like to point out that in our attempts to account for behavior of the growth twin midrib in our laminate, we witness a wave of magnetization reversal propagate across the domain. This is first evidence that we are able to achieve some progress here.

We have developed a model to understand the metastability in the computation. Let us explain the basis of this model with the comment that we have attempted to confine ourselves to what we perceived the strategic essentials: a stored energy of deformation and magnetization, a demagnetization or induced magnetic field energy, and a simple magnetic loading program intended to represent behavior when a device is subjected to a slowly oscillating field, e.g., 60 hz. If there were no demagnetization field, one would anticipate the evolution of the system to resemble that of a single magnetic particle, as described by Stoner and Wohlfarth [25]. Our idea is to derive a shadow energy that will accumulate the effects of the oscillatory behavior resulting from the demagnetization field. Although the mathematics involved here is elementary, beyond some knowledge of modern partial differential equations, the idea is that the shadow energy serves as a model of the complex simulation, just as formulating balance laws or energy principles serves as model for a physical process.

We introduce a two dimensional energy density based on a three dimensional linear elastic density with magnetic easy axes parallel to the $\langle 111 \rangle$ directions. The three dimensional density is projected onto the (0-11) plane containing the [-211] rod axis. Then we ignore out of plane strains and magnetizations. Note that the [111] and [-111] easy axes lie in the plane of projection. After performing these computations, we relabel axes in our two dimensional configuration so that $e_1 = (1,0)$ and $e_2 = (0,1)$ correspond to the [111] and [-211] directions. In these coordinates, the [111] easy axis becomes $e_2$ and the [-111] easy axis becomes $q = (\frac{2\sqrt{2}}{3}, \frac{1}{3})$. Set

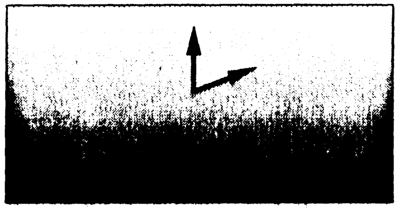

Figure 1a Single crystal with magnetic easy axes.

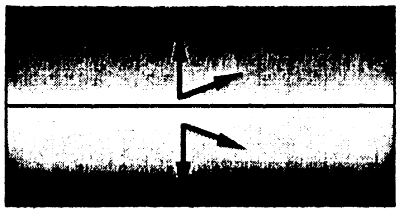

Fig 1b Growth twin laminate with magnetic easy axes.

(ii) *single crystal with demagnetization energy* The configuration destabilizes from the precursor prior to $H_{1cr}$ and descends gradually through the shoulder regime achieving absolute minimum slightly after $H_{2cr}$

(iii) *growth twin laminate with demagnetization energy* The configuration destabilizes from the precursor subsequent to passing the field value $H_{1cr}$ achieving absolute minimum slightly beyond $H_{2cr}$..

(iv) *growth twin laminate with demagnetization energy and constrained growth twin boundary* The general features are the same as in (iii) with a somewhat smoother ascent to $H_{2cr}$. The magnetostrictive strain is diminished.

We are able to provide a qualitative comparison with experiment. Material parameters useful for a more detailed comparison are not available. The computed curves in Figure 2



bear a strong resemblence to the experimental curve [6]. The strain increases with increasing positive and negative applied field and has the butterfly structure characteristic of this material. The $\lambda$–jumping described in [2] is evident in the steep section of the curve, although this is less pronounced in the experimental picture. In [7], an unbiased rod achieves about 66% of its maximum magnetostrictive strain according to one of the authors. In our simulation we achieve about 50%, which leads us to believe that our choices of parameters are reasonable.

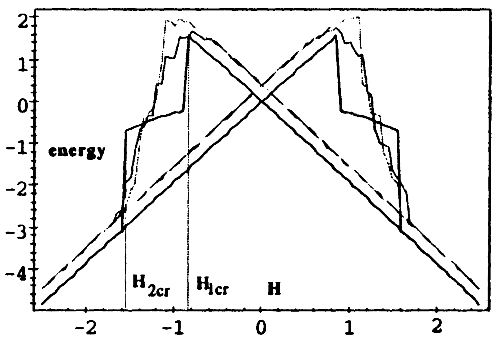


Figure 2. Energy portraits: without demagnetization energy (lowest curve), single crystal with demagnetization energy (intermediate curve), and laminate with demagnetization energy (top curve). Critical fields are labeled.

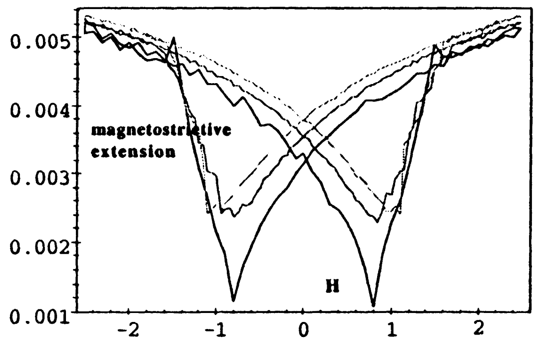


Figure 3. Magnetostriction curves: without demagnetization energy (lowest curve), single crystal with demagnetization energy (intermediate curve), and laminate with demagnetization energy (top curve).

Let $\alpha^{\circ}$ be a given magnetization, perhaps depending on H or other parameters, and let

$$\alpha^{h} = \alpha^{\circ}\chi_{\Omega} + (\xi - \alpha^{\circ})\chi_{D}, \quad |\xi| = 1, \quad D = (0,h)\times(0,1)\cup(L-h,L)\times(0,1), \tag{3.1}$$

where $h > 0$, be a variation of $\alpha^{\circ}$. We shall interpret $\alpha^{\circ}$ as a suitably stable precursor.

The energy of the system is given by

$$E(H,\alpha) = E(H,\alpha^{\circ}) + |D|\frac{E(H,\alpha) - E(H,\alpha^{\circ})}{|D|}.$$

Our shadow energy $E_{sh}$ is given by

$$E_{sh}(H,\alpha^{\circ},\xi) = E(H,\alpha^{\circ}) + \Psi^{\circ}(H,\alpha^{\circ},\xi)\,|D|, \tag{3.2}$$

$$\Psi^{\circ}(H,\alpha^{\circ},\xi) = \lim_{h\to 0}\frac{E(H,\alpha) - E(H,\alpha^{\circ})}{|D|} = \lim_{h\to 0}\Psi^{h}(H,\alpha^{\circ},\xi), \quad \text{where}$$

$$\Psi^{h}(H,\alpha^{\circ},\xi) = \varphi(\xi) - \varphi(\alpha^{\circ}) - H\cdot(\xi - \alpha^{\circ}) + \frac{1}{2h}\frac{1}{2}\int_{R^2}(|\nabla u|^2 - |\nabla u^{\circ}|^2)\,dx, \tag{3.3}$$

with

$$\Delta u = \operatorname{div}\alpha^{h}\chi_{\Omega} \text{ in } R^2 \text{ and } \Delta u^{\circ} = \operatorname{div}\alpha^{\circ}\chi_{\Omega} \text{ in } R^2.$$

The essence of the problem is to evaluate with care the demagnetization term. Note that from the differential equation we obtain that

$$\int_{R^2}(|\nabla u|^2 - |\nabla u^{\circ}|^2)\,dx = \int_D \nabla(u + u^{0})\cdot(\xi - \alpha^{\circ})\,dx$$

We suppose $\alpha^{\circ}$ and $\xi$ to be independent of $x \in D$. Introduce the auxiliary functions $w_j$ and $v_j^{(h)}$ as the solutions of the equations

$$\Delta w_j = \frac{\partial}{\partial x_j}\chi_{\Omega} \text{ and } \Delta v_j^{(h)} = \frac{\partial}{\partial x_j}\chi_{D} \quad \text{in } R^2,\ j = 1,2.$$

Moreover, we shall need explicit representations for $\partial w_1/\partial x_1$ and $\partial v_1^{(h)}/\partial x_1$. These are given by the classical Plemelj formulas [24]. Namely, in the case at hand, if $w$ denotes the solution of

$$\Delta w = \frac{\partial}{\partial x_1}\chi_{A} \text{ in } R^2, \text{ where } A \text{ is a rectangle with sides} \parallel \text{to the axes,}$$

then $(z = x_1 + ix_2)$,

$$\frac{\partial w}{\partial z}(z) = \frac{1}{2\pi i}\int_{\Gamma_1\cup\Gamma_2}\frac{dt}{t - z}, \text{ where } \Gamma_1 \text{ and } \Gamma_2 \text{ are the vertical sides.}$$

So



$$\frac{\partial w}{\partial x_1}(z) = \operatorname{Re}\frac{1}{2\pi i}\int_{\Gamma_1\cup\Gamma_2}\frac{dt}{t - z} = \frac{1}{2\pi}(\theta_1(z) + \theta_2(z)), \tag{3.4}$$

where $\theta_j(z)$ is the angle subtended by $z$ and $\Gamma_j$.

Returning to (3.3), we express the field potential

$$u = u^{\circ} + (\xi_1 - \alpha_1^{\circ})v_1^{(h)} + (\xi_2 - \alpha_2^{\circ})v_2^{(h)} \tag{3.5}$$

which, after some manipulation, gives that

$$\nabla(u + u^{0})\cdot(\xi - \alpha^{\circ}) = 2\alpha_1^{\circ}(\xi_1 - \alpha_1^{\circ})\frac{\partial w_1}{\partial x_1} + 2\alpha_2^{\circ}(\xi_2 - \alpha_2^{\circ})\frac{\partial w_2}{\partial x_2}$$

$$+ (\xi_1 - \alpha_1^{\circ})^2\frac{\partial v_1^{(h)}}{\partial x_1} + (\xi_2 - \alpha_2^{\circ})^2\frac{\partial v_2^{(h)}}{\partial x_2} + I, \quad \text{where} \int_D I\,dx = 0,$$

by symmetry. From (3.4) we observe that

$$\lim_{h\to 0}\frac{1}{|D|}\int_D\frac{\partial v_1^{(h)}}{\partial x_1}dx = 1 \quad \text{and} \quad \lim_{h\to 0}\frac{1}{|D|}\int_D\frac{\partial v_2^{(h)}}{\partial x_2}dx = 0.$$

We introduce a domain dependent "magic number" $\lambda$ by

$$\lambda = \int_{\Gamma_1}\frac{\partial w_1}{\partial x_1}dx_2 = \lim_{h\to 0}\frac{1}{|D|}\int_D\frac{\partial w_1}{\partial x_1}dx, \tag{3.6}$$

so in particular, by (3.4) again,

$$1 - \lambda = \int_{\Gamma_1}\frac{\partial w_2}{\partial x_2}dx_2 = \lim_{h\to 0}\frac{1}{|D|}\int_D\frac{\partial w_2}{\partial x_2}dx.$$

We then obtain for the demagnetization portion of the shadow energy,

$$\Psi^{\circ}_{demag}(H,\alpha^{\circ},\xi) = \lim_{h\to 0}\frac{1}{|D|}\frac{1}{2}\int_{R^2}(|\nabla u|^2 - |\nabla u^{\circ}|^2)\,dx$$

$$= \alpha_1^{\circ}(\xi_1 - \alpha_1^{\circ})\lambda + \alpha_2^{\circ}(\xi_2 - \alpha_2^{\circ})(1 - \lambda) + \tfrac{1}{2}(\xi_1 - \alpha_1^{\circ})^2 \tag{3.7}$$

[20] Kinderlehrer, D. and Ma, L. 1994 Computational hysteresis in modeling magnetic systems, IEEE Trans Mag.,30.6, 4380-4382

[21] Kinderlehrer, D. and Ma, L. 1994 Simulation of hysteresis in nonlinear systems, Math. and Control in Smart Structures, Proc. SPIE vol. 2192, (Banks, H.T.,ed.), 78-87

[22] Kinderlehrer, D. and Ma., L. The hysteretic event in magnetic systems, J. Nonlinear Science(to appear).

[23] Kinderlehrer, D. and Ma., L. The hysteretic event in the computation of magnetization and magnetostriction, Nonlinear PDE and their applications, (Brezis, H. and Lions, J.-L.,eds) Collège de France Sem vol XI, Pit. Res Notes Math Sci (to appear).

[24] Muskhelishvili, N. I. 1992 *Singular Integral Equations*, Dover (reprint of 1953 Noordhoff edition)

[25] Stoner, E. C. and Wohlfarth, E. P. 1948 A mechanisim of magnetic hysteresis in heterogeneous alloys, Phil. Trans. Royal Soc. (London) Sect A, 240, 599-642

[26] Tickle, R. Observations of the microstructure of TbxDy1−xFe2, x ≈ 0.3, under applied field and stress, MS. Thesis, University of Minnesota, in progress

[27] Wutting, M., Su, Q., Zheng, Y., and Wen, Y. 1995 Magneto-mechanical instability in Terfenol-D films, Appl. Phys. Lett. 67, 3641-3643



x